Ships advancing near the critical speed in a shallow channel with a randomly uneven bed

MOHAMMAD-REZA ALAM[1] AND CHIANG C. MEI[2]

[1]Department of Mechanical Engineering, Massachusetts Institute of Technology, Cambridge, MA 02139, USA

[2]Department of Civil and Environmental Engineering, Massachusetts Institute of Technology, Cambridge, MA 02139 USA

Effects of random bathymetric irregularities on wave generation by transcritical ship motion in a shallow channel are investigated. Invoking Boussinesq approximation in shallow waters, it is shown that the wave evolution is governed by an integro-differential equation combining features of Korteweg–deVries and Burgers equations. For an isolated ship, the bottom roughness weakens the transient waves radiated both fore and aft. When many ships advance in tandem, a steady mount of high water can be formed in front and a depression behind. Wave forces on both an isolated ship and a ship in a caravan are obtained as functions of the mean-square roughness, ship speed and the blockage coefficient.

1. Introduction

With increasing numbers of high-speed ferries, marine accidents are of serious concern to several ports and seaways in the world. Large waves like 'the white cliffs of Dover' caused by a fast catamaran have been blamed for the death of a victim overthrown from another fishing boat, near the Port of Harwich, UK. There have been strong indications that these waves are close to solitary waves known to appear ahead of a ship advancing near the critical speed (linearized long-wave speed) in a channel (Hamer 1999).

An unusual characteristic of the upstream solitons is that they are the unsteady response to steady forcing, unlike the transonic flow in compressible aerodynamics. Although noted long ago in tank experiments by Thews & Landweber (1935), scientific interest was renewed by laboratory observations of ship-induced solitons by Ertekin, Webster & Wehausen (1986). Theoretical elucidations were started by Wu & Wu (1982) who studied the two-dimensional problem (vertical and horizontal) by numerical solution of the one-dimensional Boussinesq approximation which includes weak nonlinearity and dispersion, for waves generated by a moving surface pressure. For a moving point disturbance, Akylas (1984) showed that the free-surface elevation is governed by the forced Korteweg–deVries equation. A similar two-dimensional analysis for a bottom obstacle was made by Cole (1985).

An upstream soliton due to a slender ship in a channel is a three-dimensional problem. Asymptotic theories have been given by Mei (1986) for a thin strut, and for a slender ship in a channel with a flat bottom by Mei & Choi (1987). Their studies were confined to a narrow channel so that the disturbances both fore and aft are one-dimensional. Choi & Mei (1989) further studied a wide channel in which the waves in

the wake are fully two-dimensional and must be treated by the Kadomtsev–Petviashvili (K-P) equation . Further extensions have been reported by Chen & Sharma (1995) who considered a ship moving parallel to the sidewalls but off the centreline of the channel, and took into account more realistic geometry of the ship hull. Li & Sclavounos (2002) examined numerically ship-induced waves in an unbounded shallow sea. They found that wave crests radiated upstream are no longer straight, but are parabolic. By direct numerical simulation, Zhang & Chwang (2001) solved the full Euler's equations for the transcritical flow over a semi-infinite step facing either forward or backward, and found an upstream- or a downstream-propagating undular bore.

The effects of a randomly uneven seabed of intermediate depth have been studied for free nonlinear surface waves without ships by Mei & Hancock (2003) and Pihl, Mei & Hancock (2002). They have shown that the envelope of narrow-banded waves obeys an extended nonlinear Schrödinger equation with a complex damping term. For long waves in shallow seas, harmonic generation and localization have been examined by Grataloup & Mei (2003), and soliton localization by Mei & Li (2004), both for a homogeneous fluid layer. Extension to interfacial waves in a two-layered sea has been reported by Alam & Mei (2007).

In this paper, we examine ship-generated waves in a shallow channel with a randomly uneven bed, when the ship speed is near-critical. The present work is a combination of Mei (1986) and Mei & Choi (1987) on upstream radiation of solitons over a smooth bed, and of Mei & Li (2004) on soliton propagation over a randomly rough bed. Our objectives are to examine how disorder affects the stochastic mean quantities such as the free-surface profiles and the wave forces on a ship. Results are discussed for an isolated ship as well as a caravan of identical ships travelling at the same speed.

2. Exact formulation

Let the channel be of nearly rectangular cross-section with uniform width $2W$ and constant mean depth H_0. In the stationary frame of reference (x^*, y^*, z^*), the channel depth $H^*(x^*)$ deviates slightly from the mean by a one-dimensional random fluctuation $h^*(x^*)$ so that $H^*(x^*) = H_0 - h^*(x^*)$ where $h^*(x^*) \ll H_0$. A ship of length $2L$ advances at a constant speed U along the centreline of the channel in the direction of the positive x^*-axis. Assuming symmetry, only half of the channel width need be considered.

For treating the neighbourhood of the ship, it is convenient to use the ship-bound coordinates $(\xi^* = x^* - Ut^*, y^*, z^*)$. In dimensional terms, the three-dimensional velocity potential Φ^* satisfies

$$\Phi^*_{\xi^*\xi^*} + \Phi^*_{y^*y^*} + \Phi^*_{z^*z^*} = 0, \tag{2.1}$$

in the fluid $(-H^* < z^* < \zeta^*)$, and

$$\Phi^*_{z^*} = \zeta^*_{t^*} + (-U + \Phi^*_{\xi^*})\zeta^*_{\xi^*} + \zeta^*_{y^*}\Phi^*_{y^*}, \tag{2.2}$$

$$g\zeta^* + \Phi^*_{t^*} - U\Phi^*_{\xi^*} + \tfrac{1}{2}[(\Phi^*_{\xi^*})^2 + (\Phi^*_{y^*})^2 + (\Phi^*_{z^*})^2] = 0, \tag{2.3}$$

on the free surface $(z^* = \zeta^*)$, and

$$\Phi^*_{y^*} = 0, \quad y^* = W, \tag{2.4}$$

on the channel bank. No flux across the ship hull $r^* = \sqrt{y^{*2} + z^{*2}} = R^*(\xi^*, \theta)$ requires

$$\frac{\partial \Phi^*}{\partial n^*} = (-U + \Phi^*_{\xi^*})\frac{R^*_{\xi^*}}{\sqrt{1 + R^{*2}_\theta/R^{*2}}}, \quad r^* = R^*(\xi^*, \theta). \tag{2.5}$$

where r^* and θ are polar coordinates in the (x^*, y^*)-plane. In moving coordinates, the bed condition is

$$\frac{\partial \Phi^*}{\partial z^*} = H_{\xi^*}^* \Phi_{\xi^*}^*, \quad z^* = -H^*(x^*) = -H^*(\xi^* + Ut^*). \tag{2.6}$$

It is assumed that $H^*(x^*)$ is a random function of x^* with constant mean H_0.

For treating the waves far away from the ship, we shall later employ the stationary coordinates and assume weak nonlinearity and dispersion:

$$\epsilon \equiv \frac{A}{H_0} \ll 1, \quad \mu \equiv \frac{H_0}{L} \ll 1 \quad \text{with} \quad \epsilon = O(\mu^2), \tag{2.7}$$

where A denotes the characteristic wave amplitude. As in Mei & Choi (1987), we also assume that the channel width is comparable to ship length,

$$\frac{L}{W} = \gamma = O(1), \tag{2.8}$$

and that the ship is slender so that the characteristic radius of the cross-section R_0, defined by $\pi R_0^2 = S_0$ where S_0 is the maximum area of the cross-section, is small compared to the length L, so that the slenderness ratio is

$$\delta \equiv \frac{R_0}{L} = O(\mu^{5/2}) \ll 1 . \tag{2.9}$$

The blockage coefficient, defined as the ship-to-channel ratio of cross-sectional areas, is of the order

$$C_B \equiv \frac{S_0}{2WH_0} = \frac{\pi R_0^2}{2WH_0} \sim \frac{R_0^2}{L^2} \frac{L^2}{WH_0} \sim O(\mu^4). \tag{2.10}$$

The method of matched asymptotics will be employed. Accordingly, the cross-section of the rectangular channel is separated into three regions around a ship. In the ship-bound coordinate, they are distinguished by:

   (*a*) the near field: $|\xi^*| \leqslant O(L), (y^*, z^*) = O(R_0)$,

   (*b*) the intermediate field: $|\xi^*| \leqslant O(L), (y^*, z^*) = O(H_0)$,

   (*c*) the far field: $|\xi^*| \geqslant O(L), y^* = O(W) \gg O(H_0), z^* = O(H_0)$.

For a ship advancing in shallow water, waves in the far field are essentially two-dimensional in the horizontal plane and forced by the outward mass flux due the bow-to-stern variation of the hull. We first sketch the derivation of the mass flux from the near and intermediate fields in order to provide a lateral boundary condition for the far field. Since the details are closely similar to Mei & Choi (1987), only the key results are given here for clarity.

3. Near field

Since the bed is outside the near field, the bed roughness does not enter the near-field analysis. Let the dimensionless near-field variables be defined by

$$\Phi^* = \frac{AL\sqrt{gH_0}}{H_0}\Phi, \quad \zeta^* = A\zeta, \quad \xi^* = L\xi, \quad (y^*, z^*, r^*) = R_0(\hat{y}, \hat{z}, \hat{r}), \quad t^* = \frac{L\hat{t}}{\sqrt{gH_0}}. \tag{3.1}$$

Hereinafter, we shall choose A so that $\epsilon = \mu^2$. Laplace's equation becomes

$$\delta^2 \Phi_{\xi\xi} + \Phi_{\hat{y}\hat{y}} + \Phi_{\hat{z}\hat{z}} = 0, \quad -\infty < \hat{z} < \frac{\mu^3}{\delta}\zeta, \tag{3.2}$$

where $\mu^3/\delta = O(\mu^{1/2})$. The normalized kinematic and dynamic conditions on the surface read:

$$\Phi_{\hat{z}} = \mu\delta\zeta_{\hat{t}} + \mu\delta(-\mathscr{F} + \Phi_{\xi})\zeta_{\xi} + \frac{\mu^3}{\delta}\Phi_{\hat{y}}\zeta_{\hat{y}}, \quad \hat{z} = \frac{\mu^3}{\delta}\zeta, \tag{3.3}$$

$$\Phi_{\hat{t}} + \zeta - \mathscr{F}\Phi_{\xi} + \frac{\mu^2}{2}\left[(\Phi_{\xi})^2 + \frac{1}{\delta^2}(\Phi_{\hat{y}})^2 + \frac{1}{\delta^2}(\Phi_{\hat{z}})^2\right] = 0, \quad \hat{z} = \frac{\mu^3}{\delta}\zeta, \tag{3.4}$$

where $\mathscr{F} = U/\sqrt{gH_0}$ is the Froude number. On the ship hull we have

$$\frac{\partial\Phi}{\partial n} = \left(\frac{\delta}{\mu}\right)^2 (-\mathscr{F} + \mu^2\Phi_{\xi})\frac{R_{\xi}}{\sqrt{1 + (R_{\theta}/R)^2}}. \tag{3.5}$$

Note that $(\delta/\mu)^2 = O(\mu^3)$. By Taylor approximation about the mean sea level and introducing expansions

$$\Phi = \Phi^{(0)} + \mu^2\Phi^{(2)} + \left(\frac{\delta}{\mu}\right)^2\Phi^{(3)} + \cdots, \qquad \zeta = \zeta^{(0)} + \mu^2\zeta^{(2)} + \left(\frac{\delta}{\mu}\right)^2\zeta^{(3)} + \cdots, \tag{3.6}$$

Mei & Choi (1987) have shown that the near-field solution is quasi two-dimensional in the cross-sectional plane

$$\Phi = f^{(0)} + \mu^2 f^{(2)} + \frac{\delta^2}{\mu^2}\left[f^{(3)} + \frac{q}{\pi}\ln\left(\frac{\delta}{\mu}\hat{r}\right)\right] + \cdots, \tag{3.7}$$

where q amounts to the radial flux caused by the changing cross-section from bow to stern, and is related to the cross-sectional area of the hull $S^* = S_0 S(\xi)$ by

$$q = \frac{2}{\gamma}\frac{\mu}{\delta^2}C_B S_{\xi} = O(1), \tag{3.8}$$

where C_B is the blockage coefficient defined in (2.10). Equation (3.7) will provide a condition for matching with the intermediate field at $O(\mu^3)$. The functions $f^{(0)}, f^{(2)}, f^{(3)}$ depend only on $\hat{x}, \hat{t}$ and contribute only to the wave force in the ship. Note that the results in this section are deterministic.

4. Intermediate field

Renormalizing only the lateral coordinates

$$(y^*, z^*, h^*) = H_0(\bar{y}, \bar{z}, h), \quad H^* = H_0 H, \tag{4.1}$$

while keeping all other variables the same, we rewrite (2.1) as

$$\mu^2\Phi_{\xi\xi} + \Phi_{\bar{y}\bar{y}} + \Phi_{\bar{z}\bar{z}} = 0 \quad \text{in the fluid} \tag{4.2}$$

and (2.2) and (2.3) as,

$$\Phi_{\bar{z}} = \mu^2[\zeta_{\hat{t}} - \mathscr{F}\zeta_{\xi}] + \mu^4\zeta_{\xi}\Phi_{\xi} + \mu^2\zeta_{\bar{y}}\Phi_{\bar{y}}, \quad \bar{z} = \mu^2\zeta, \tag{4.3}$$

$$\Phi_t + \zeta - \mathscr{F}\Phi_{\xi} + \tfrac{1}{2}\left(\mu^2\Phi_{\xi} + \Phi_{\bar{y}} + \Phi_{\bar{z}}^2\right) = 0, \quad \bar{z} = \mu^2\zeta. \tag{4.4}$$

For the uneven seabed, we shall assume, as in Mei & Li (2004), that the depth deviates slightly from a constant mean:

$$H(x) = 1 - \mu h(x), \quad \text{i.e.} \quad H(\xi + \mathscr{F}t) = 1 - \mu h(\xi + \mathscr{F}t), \tag{4.5}$$

where $x = x^*/L$. On the channel bed, we have

$$\Phi_{\bar{z}} = \mu^3 h_{\xi}\Phi_{\xi}, \quad \bar{z} = -1 + \mu h, \tag{4.6}$$

where $h = h(x)$ is random in x with zero mean. Clearly, $h_x = h_\xi$. In view of (3.7), the intermediate field is driven by a line source, and also affected at the bottom by a random disturbance. Both effects occur at $O(\mu^3)$.

Again by assuming expansions in the form of (3.6), a sequence of linear boundary-value problems is obtained. At $O(\mu^0)$ and $O(\mu^2)$, the solutions are not affected by the bed roughness, nor by the line source, hence are deterministic. At $O(\mu^3)$, $\Phi^{(3)}$ is the sum of a deterministic part and a stochastic part. The two parts can be solved separately because of linearity. Since the right-hand side of (4.6) has zero stochastic mean, $\langle \Phi^{(3)} \rangle$ is driven only by the line source from the near field. Hence, the solution is the same as that for a smooth bed derived by Mei & Choi (1987). For matching with the far field, we cite its outer approximation ($\bar{y} \gg 1$)

$$\langle \Phi \rangle \approx f^{(0)} + \mu f^{(1)} + \mu^2 \left[f^{(2)} - \tfrac{1}{2}(z+1)^2 f^{(0)}_{zz} \right] + \left(\frac{\delta}{\mu} \right)^2 \left(f^{(3)} + \tfrac{1}{2} q \bar{y} \right). \tag{4.7}$$

At large $\bar{y}$, the stochastic mean of the lateral flux is therefore,

$$\langle \Phi_{\bar{y}} \rangle \approx \left(\frac{\delta}{\mu} \right)^2 \tfrac{1}{2} q = \frac{C_B S_\xi(\xi)}{\gamma \mu}, \quad \bar{y} = \frac{y^*}{H_0} \gg 1, \tag{4.8}$$

which will give the boundary condition for the far field on $y = 0$.

5. The far field and the wave forces

In view of the assumption (2.7), the approximate Boussinesq equations apply in the far field for the free-surface displacement and the depth-averaged horizontal velocity $\boldsymbol{u}^* = (u^*, v^*) = (\phi_x^*, \phi_y^*)$, where ϕ^* is the depth-averaged potential.

Here, it is natural to use the stationary coordinates system. Let the following dimensionless variables be introduced:

$$x^* = Lx, \quad y^* = Wy, \quad (z^*, H^*) = H_0(z, H), \quad t^* = \frac{tL}{\sqrt{gH_0}}, \tag{5.1a}$$

$$(u^*, v^*) = (u, v) \frac{A}{H_0} \sqrt{gH_0}, \quad \phi^* = \frac{AL\sqrt{gH_0}}{H_0} \phi, \quad \zeta^* = A\zeta, \tag{5.1b}$$

so that $(u, v) = (\phi_x, \phi_y)$. The dimensionless Boussinesq equations are

$$\frac{\partial \zeta}{\partial t} + \nabla \cdot [(H + \epsilon \zeta) \boldsymbol{u}] = 0 \tag{5.2}$$

$$\frac{\partial \boldsymbol{u}}{\partial t} + \epsilon \boldsymbol{u} \cdot \nabla \boldsymbol{u} + \nabla \zeta = \mu^2 \frac{H}{2} \nabla \left[\nabla \cdot \left(H \frac{\partial \boldsymbol{u}}{\partial t} \right) \right] - \mu^2 \frac{H^2}{6} \nabla \left(\nabla \cdot \frac{\partial \boldsymbol{u}}{\partial t} \right) \tag{5.3}$$

where $\nabla = (\partial/\partial x, \gamma \partial/\partial y)$.

For a randomly uneven seabed, as in Mei & Li (2004), we assume that the slight deviation from a constant mean $h(x)$ is stationary random with zero mean and known covariance,

$$\langle h(x) \rangle = 0, \quad \langle h(x)h(x') \rangle = \Gamma(|x - x'|). \tag{5.4}$$

Our attention will be focused on the neighbourhood of the critical speed, i.e.

$$\mathscr{F} \equiv \frac{U}{\sqrt{gH_0}} = 1 - \alpha \mu^2, \tag{5.5}$$

where the coefficient $\alpha = O(1)$ can be positive (negative) if the ship speed is subcritical (supercritical).

Alternatively, Bernoulli's equation can be derived from (5.3), and then combined with the continuity equation (5.2) to give a single equation for ϕ, with a stochastic coefficient h:

$$\nabla^2\phi - \frac{\partial^2\phi}{\partial t^2} - \frac{\epsilon}{2}\frac{\partial}{\partial t}(\nabla\phi)^2 - \epsilon\nabla\cdot\left(\frac{\partial\phi}{\partial t}\nabla\phi\right) + \frac{\mu^2}{3}\nabla^2\frac{\partial^2\phi}{\partial t^2} - \mu\nabla\cdot(h\nabla\phi) = 0. \quad (5.6)$$

On the channel bank $y = 1$, the boundary condition is

$$\phi_y = 0, \quad -\infty < x < \infty, \quad y = 1. \quad (5.7)$$

On the ship path, the boundary condition for the stochastic mean is, by matching with the intermediate field and using (3.8),

$$\langle\phi_y\rangle = \frac{1}{\mu\gamma}\langle\Phi_y\rangle = \frac{C_B S_\xi}{\mu^2\gamma^2} = O(\mu^2), \quad y \cong 0, \quad (5.8)$$

since $\bar{y} = y/\mu\gamma$. In view of the small departure from the critical speed, slow transients are anticipated. Using two time variables t and $\tau = \mu^2 t$ we assume a two-time expansion for ϕ

$$\phi = \phi_0(x, y, t, \tau) + \mu\phi_1(x, y, t, \tau) + \mu^2\phi_2(x, y, t, \tau) + \cdots, \quad \tau = \mu^2 t. \quad (5.9)$$

The following perturbation equations are derived for $O(1, \mu, \mu^2)$:

$$\left(\frac{\partial^2}{\partial x^2} + \gamma^2\frac{\partial^2}{\partial y^2} - \frac{\partial^2}{\partial t^2}\right)\phi_0 = 0, \quad (5.10)$$

$$\left(\frac{\partial^2}{\partial x^2} + \gamma^2\frac{\partial^2}{\partial y^2} - \frac{\partial^2}{\partial t^2}\right)\phi_1 = \frac{\partial}{\partial x}\left(h\frac{\partial\phi_0}{\partial x}\right) + \gamma^2 h\frac{\partial^2\phi_0}{\partial y^2}, \quad (5.11)$$

$$\left(\frac{\partial^2}{\partial x^2} + \gamma^2\frac{\partial^2}{\partial y^2} - \frac{\partial^2}{\partial t^2}\right)\phi_2 = 2\frac{\partial^2\phi_0}{\partial t\partial\tau} + \frac{1}{2}\frac{\partial}{\partial t}(\nabla\phi_0)^2 + \nabla\cdot\left(\frac{\partial\phi_0}{\partial t}\nabla\phi_0\right)$$
$$- \frac{1}{3}\nabla^2\frac{\partial^2\phi_0}{\partial t^2} + \frac{\partial}{\partial x}\left(h\frac{\partial\phi_1}{\partial x}\right) + \gamma^2 h\frac{\partial^2\phi_1}{\partial y^2}. \quad (5.12)$$

Along the channel bank, we have

$$\frac{\partial\phi_0}{\partial y} = \frac{\partial\phi_1}{\partial y} = \frac{\partial\phi_2}{\partial y} = 0, \quad y = 1. \quad (5.13)$$

Along the centreline (the ship path), we require

$$\frac{\partial\phi_0}{\partial y} = \frac{\partial\phi_1}{\partial y} = 0, \quad y = 0. \quad (5.14)$$

At $O(\mu^2)$, only the stochastic averages are required,

$$\frac{\partial\langle\phi_2\rangle}{\partial y} = \frac{C_B}{\gamma^2\mu^4}S_x, \quad y = 0, \quad (5.15)$$

where $S_x \equiv 0$ for $|x - \mathscr{F}t| > 1$. At leading order, the governing equation for ϕ_0 is homogeneous. Owing to the boundary condition, (5.13), (5.14), it can be shown that the solution for ϕ_0 is one-dimensional (independent of y). Focusing attention on waves advancing forward with the ship, we take

$$\phi_0 = \phi_0(\sigma, \tau), \quad (5.16)$$

where $\sigma = x - t$ is the characteristic coordinate.

At $O(\mu)$, the equation for ϕ_1 is inhomogeneous. The second forcing term on the right-hand side of (5.11) is identically zero. The first term is random with zero mean.

Hence, the response is likewise stochastic with zero mean,

$$\phi_1 = - \int_{-\infty}^{t} dt' \int_{-\infty}^{\infty} dx' G(x,t;x',t') \frac{\partial}{\partial x'} \left(h(x') \frac{\partial \phi_0(x'-t',\tau)}{\partial x'} \right), \qquad (5.17)$$

where

$$G(x,t;x',t') = -\tfrac{1}{2}\mathscr{H}[(t-t') - |x-x'|], \qquad (5.18)$$

is Green's function with $\mathscr{H}$ denoting the Heaviside step function (Duffy 2001, §3.1, p. 78).

We next take the stochastic average of (5.12) and integrate the result with respect to y from 0 to 1. Applying the boundary condition (5.15), we obtain an inhomogeneous equation for $\bar{\phi}_2 = \int_0^1 \phi_2 dy$ which is the cross-channel average of ϕ_2,

$$\frac{\partial^2 \langle \bar{\phi}_2 \rangle}{\partial x^2} - \frac{\partial^2 \langle \bar{\phi}_2 \rangle}{\partial t^2} = 2 \frac{\partial^2 \phi_0}{\partial t \partial \tau} + \frac{C_B}{\mu^4} S_x + \frac{1}{2} \frac{\partial}{\partial t} \left(\frac{\partial \phi_0}{\partial x} \right)^2$$

$$+ \frac{\partial}{\partial x} \left(\frac{\partial \phi_0}{\partial t} \frac{\partial \phi_0}{\partial x} \right) - \frac{1}{3} \frac{\partial^4 \phi_0}{\partial x^2 \partial t^2} + \frac{\partial}{\partial x} \left\langle h \frac{\partial \phi_1}{\partial x} \right\rangle, \quad (5.19)$$

The last term on the right-hand side of (5.19) can be evaluated as in Mei & Li (2004)(equations 18–22, 24–29) to give

$$\frac{\partial}{\partial x} \left\langle h(x) \frac{\partial \phi_1}{\partial x} \right\rangle = 2 \frac{\partial}{\partial \sigma} \left\{ \frac{\Gamma(0)}{2} \frac{\partial \phi_0}{\partial \sigma} + \frac{\hat{\Gamma}(0)}{8} \frac{\partial^2 \phi_0}{\partial \sigma^2} + \frac{1}{16} \int_{-\infty}^{\infty} \Gamma \left(\frac{\sigma - \sigma'}{2} \right) \right.$$

$$\left. \times \frac{\partial^2 \phi_0}{\partial \sigma'^2} d\sigma' + \frac{1}{8} \int_{-\infty}^{\infty} P \left(\frac{\sigma - \sigma'}{2} \right) \frac{\partial^3 \phi_0}{\partial \sigma'^3} d\sigma' \right\} \quad (5.20)$$

where $\hat{\Gamma}$ is the Fourier transform of the covariance Γ and

$$P(x) = \int_{|x|}^{\infty} \Gamma(u) \, du. \qquad (5.21)$$

In particular, if the covariance is Gaussian,

$$\Gamma(x-x') = D^2 \exp \left(-\frac{(x-x')^2}{2\ell^2} \right), \qquad (5.22)$$

where D is the dimensionless root-mean-square amplitude of the random roughness and ℓ is the dimensionless correlation length (normalized, respectively, according to $\ell^* = \ell L$ and $D^* = D\sqrt{AH_0}$ or equivalently $D^* = \mu D H_0$). Equation (5.20) then takes the more explicit form (Mei & Li 2004)

$$\frac{\partial}{\partial x} \left\langle h(x) \frac{\partial \phi_1}{\partial x} \right\rangle = 2D^2 \frac{\partial}{\partial \sigma} \left\{ \frac{1}{2} \frac{\partial \phi_0}{\partial \sigma} + \frac{\sqrt{2\pi}\ell}{8} \frac{\partial^2 \phi_0}{\partial \sigma^2} + \frac{1}{16} \int_{-\infty}^{\infty} \exp \left(-\frac{|\sigma - \sigma'|^2}{8\ell^2} \right) \right.$$

$$\left. \times \frac{\partial^2 \phi_0}{\partial \sigma'^2} d\sigma' + \frac{\sqrt{2\pi}\ell}{16} \int_{-\infty}^{\infty} \mathrm{erfc} \left(\frac{|\sigma - \sigma'|}{2\sqrt{2}\ell} \right) \frac{\partial^3 \phi_0}{\partial \sigma'^3} d\sigma' \right\}. \quad (5.23)$$

All terms on the right-hand side of (5.19) are functions of $\sigma = x - t$ to the leading order, hence it satisfies the homogeneous one-dimensional wave equation. For $\langle \bar{\phi}_2 \rangle$ to be bounded, the right-hand side must vanish, yielding the evolution equation for ϕ_0.

$$0 = 2 \frac{\partial^2 \phi_0}{\partial t \partial \tau} + \frac{C_B S_x}{\mu^4} + \frac{1}{2} \frac{\partial}{\partial t} \left(\frac{\partial \phi_0}{\partial x} \right)^2 + \frac{\partial}{\partial x} \left(\frac{\partial \phi_0}{\partial t} \frac{\partial \phi_0}{\partial x} \right) - \frac{1}{3} \frac{\partial^4 \phi_0}{\partial x^2 \partial t^2} + \frac{\partial}{\partial x} \left\langle h \frac{\partial \phi_1}{\partial x} \right\rangle.$$

$$(5.24)$$

By using the zeroth-order approximations of (5.2) and (5.3), we replace $-\phi_{0,t}$ and $\phi_{0,x}$ by ζ, so that

$$\frac{\partial \zeta}{\partial \tau} + \tfrac{3}{2}\zeta\frac{\partial \zeta}{\partial x} + \frac{1}{6}\frac{\partial^3 \zeta}{\partial x^3} - \frac{1}{2}\frac{\partial}{\partial x}\left\langle h\frac{\partial \phi_1}{\partial x}\right\rangle = -\frac{1}{2}\frac{C_B S_x}{\mu^4}. \tag{5.25}$$

It is convenient to transform (5.25) further from (x, t, τ) and $(\sigma = x - t, \tau)$ to the ship-bound coordinates (ξ, τ) where $\xi = x - \mathscr{F}t = \sigma + \alpha\tau$. Since $\partial/\partial x = \partial/\partial\sigma = \partial/\partial\xi$, and $\sigma - \sigma' = \xi - \xi'$, we obtain

$$\frac{\partial \zeta}{\partial \tau} + \alpha\frac{\partial \zeta}{\partial \xi} + \tfrac{3}{2}\zeta\frac{\partial \zeta}{\partial \xi} + \frac{1}{6}\frac{\partial^3 \zeta}{\partial \xi^3} - \frac{1}{2}\frac{\partial}{\partial x}\left\langle h\frac{\partial \phi_1}{\partial x}\right\rangle = -\frac{1}{2}\frac{C_B S_\xi}{\mu^4}. \tag{5.26}$$

In the limit of a smooth bed, (5.26) reduces to the forced KdV equation of Mei (1986). Without the moving ship, the integro-differential equation for waves over a stationary random bed is recovered (Mei & Li 2004). Here, waves are forced deterministically by the ship, but their propagation is altered by the added dispersion and diffusion due to random scattering at the channel bottom.

For Gaussian correlation, we have

$$\frac{\partial \zeta}{\partial \tau} + \alpha\frac{\partial \zeta}{\partial \xi} + \frac{3}{2}\zeta\frac{\partial \zeta}{\partial \xi} + \frac{1}{6}\frac{\partial^3 \zeta}{\partial \xi^3}$$

$$- D^2\frac{\partial}{\partial \xi}\left\{\tfrac{1}{2}\zeta + \frac{\sqrt{2\pi}\ell}{8}\frac{\partial \zeta}{\partial \xi} + \frac{1}{16}\int_{-\infty}^{\infty}\exp\left(-\frac{|\xi-\xi'|^2}{8\ell^2}\right)\frac{\partial \zeta}{\partial \xi'}\,\mathrm{d}\xi\right.$$

$$\left. + \frac{\sqrt{2\pi}\ell}{16}\int_{-\infty}^{\infty}\mathrm{erfc}\left(\frac{|\xi-\xi'|}{2\sqrt{2}\ell}\right)\frac{\partial^2 \zeta}{\partial \xi'^2}\,\mathrm{d}\xi'\right\} = -\frac{\beta}{2}S_\xi \quad \text{where } \beta \equiv \frac{C_B}{\mu^4} = O(1). \tag{5.27}$$

Subject to the condition of vanishing initial data, the preceding integro-differential equation (5.27) can be numerically solved by the spectral method in a periodic domain much larger than the zone of significant motion, as in Mei & Li (2004) and Alam & Mei (2007). Note that the parameter γ does not appear. Extension to a somewhat wider channel of $W/L = O(\mu^{-1/2})$ is straightforward and leads to the same integro-differential equation.

At the leading order, the hydrodynamic pressure is the same in the near, intermediate and far fields, and is proportional to $\zeta \propto f^{(0)}$. Once the surface elevation ζ is solved from (5.27), the wave forces on the ship follow by integration over the hull. Let us define the dimensionless wave resistance, vertical lift and trim moment by

$$R_w = \frac{R_w^*}{\rho g V}, \quad F_z = \frac{F_z^*}{\rho g L A_w}, \quad M = \frac{M^*}{\rho g L^2 A_w}, \tag{5.28}$$

respectively, where V is the displaced volume of the ship, and A_w is its water-plane area. It suffices to quote from Mei & Choi (1987) (equations (7.5), (7.7), (7.9)) that

$$R_w = -\frac{\mu^3}{2C_p}\int_{-1}^{1}\zeta\frac{\mathrm{d}S}{\mathrm{d}\xi}\mathrm{d}\xi, \quad F_z = \frac{\mu^3}{2C_w}\int_{-1}^{1}\zeta Y_w\mathrm{d}\xi, \quad M = \frac{\mu^3}{2C_w}\int_{-1}^{1}\zeta Y_w\xi\mathrm{d}\xi, \tag{5.29}$$

where $Y_w(\xi)$ is the half-beam width at the water plane, C_p and C_w are, respectively, the prismatic coefficient and the waterplane area coefficient defined by

$$C_p = \frac{V}{2LS_0^*}, \quad C_w = \frac{A_w}{4BL}. \tag{5.30}$$
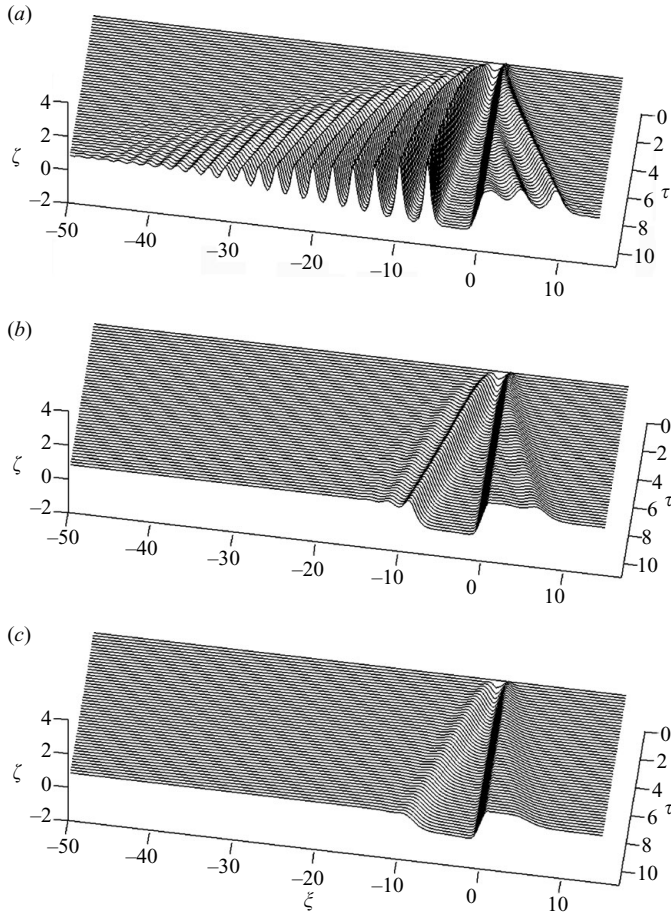
FIGURE 1. Free-surface evolution near a single slender ship moving at subcritical speed ($\alpha = 0.5$) in an infinite channel. The ship is located in the range $-1 < \xi < 1$. (*a*) $D^2 = 0$, (*b*) $D^2 = 0.5$, (*c*) $D^2 = 1$. Common parameters are $\beta = 2$, $\ell = 1$.

We now discuss the results of free-surface profiles caused by, and wave forces on, slender ships, by the numerical solution of the initial-boundary-value problem for (5.27). Such information can provide a quantitative basis for establishing new regulations for ferry operations for the safety of both the vessels and the environment.

6. Computed free-surface profiles

6.1. *One ship*

We first examine the computed results for waves generated by a single ship in an infinitely long channel. The cross-section is assumed to be a semicircle with its area varying parabolically along the ship, i.e.

$$S(\xi) = \begin{cases} 1 - \xi^2, & |\xi| < 1, \\ 0, & |\xi| > 1. \end{cases} \tag{6.1}$$

Here the spatial period (domain) for spectral computations is chosen to be sufficiently large so that no appreciable disturbances are found near the ends. Typical long-time evolution of waves are shown in figures 1–3 for $\alpha = 0.5$ (subcritical) , 0 (critical) and
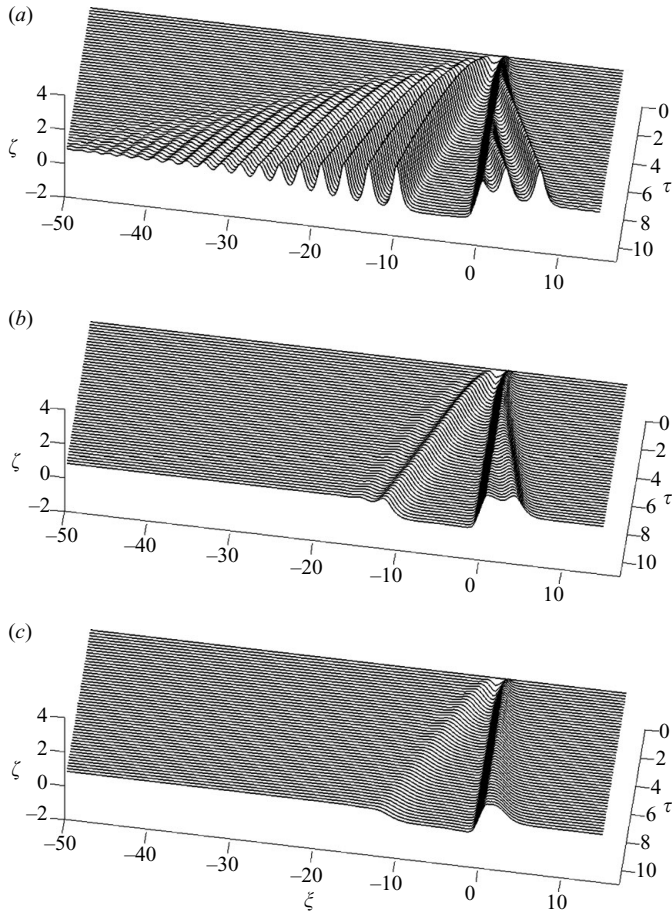
FIGURE 2. As for figure 1, but at critical speed ($\alpha = 0$).

−0.5 (supercritical) speeds. For each speed, three roughness amplitudes are chosen, $D^2 = 0$, 0.5 and 1. We fix the blockage parameter defined in (5.27) as $\beta = 2$ and the correlation length as $\ell = 1$. Over a flat bottom ($D = 0$), solitons are radiated upstream, while nearly periodic waves with diminishing amplitudes trail behind a depression in the wake. As the ship velocity increases from subcritical to supercritical values, the frequency of soliton radiation decreases while the amplitude increases (Mei 1986). Over a rough bed (finite D), the upstream waves are no longer solitons. A mound of high water is pushed forward by the bow. As D increases, waviness gradually disappears. The horizontal extent of the mound also decreases. In the ship's wake, trailing waves are found behind a stretch of depression. As the roughness increases, undulations also disappear in the wake.

6.2. *Many ships in tandem*

Results for a caravan of identical ships are more striking. We first fix the centre-to-centre separation distance to be $\Delta\xi = 20$. The ship is located in $-1 < \xi_N < 1$ where ξ_N is the centre of the Nth ship. At the critical speed $\alpha = 0$, the free-surface evolution is shown in figure 4 for three different roughnesses. Over a smooth bed, multiple reflections continue so that waves between successive ships are always transient. For small roughness height $D^2 = 0.5$, several crests riding on a high plateau are radiated

(a)

(b)

(c)
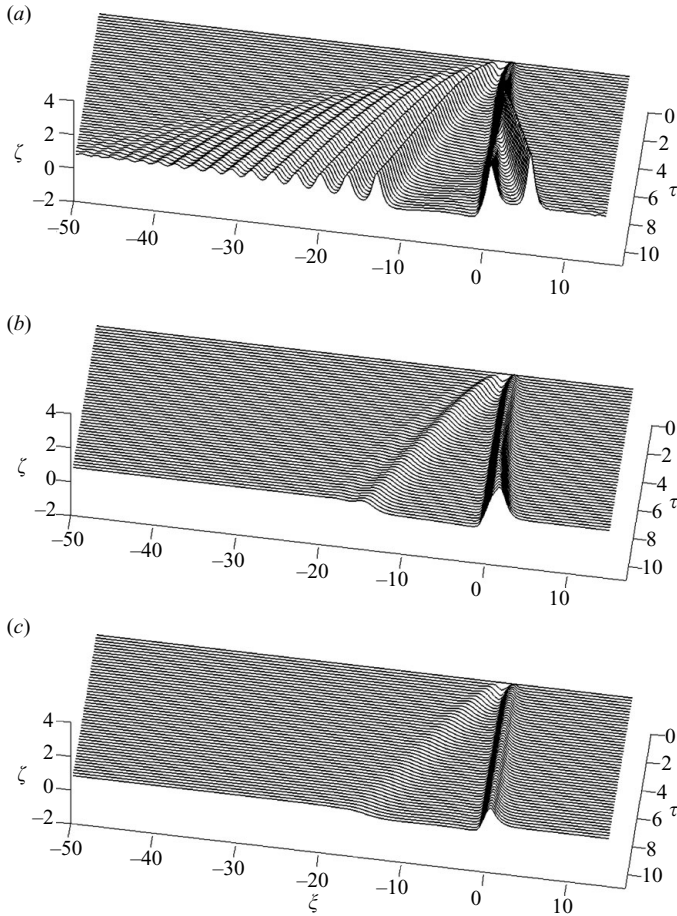
FIGURE 3. As for figure 1, but at supercritical speed ($\alpha = -0.5$).

upstream at first. After the leading crest reaches almost the mid length between two ships, all crests reach a steady state and advance at the same speed. The leading crest is the highest; the smaller ones trail behind with heights diminishing so that the free surface reduces to a flat plateau near the stern. In the wake of a ship is a depression which lengthens to join the leading crest ahead the following ship. As the roughness increases, the number of undulating crests diminishes, resulting in a flat plateau of high water ahead and a low depression behind.

The final steady wave profiles are shown in figure 5 for different roughness amplitudes. The height of the high water in front of a ship in a caravan is nearly independent of the roughness amplitude. However, the depths of the depressions behind the ships decrease as the roughness amplitude increases. Higher roughness also diminishes the undulation and the extent of the water mound in front.

The effect of the ship speed (α) is shown in figure 6. As the ship speed increases from subcritical, critical to supercritical values, the average amplitude of high water increases, but the horizontal extent decreases. The average depth of the depression behind also decreases. For the given distance between ships ($\Delta \xi = 20$), the supercritical ship has the fewest undulations on the plateau in front.

(*a*)

(*b*)

(*c*)
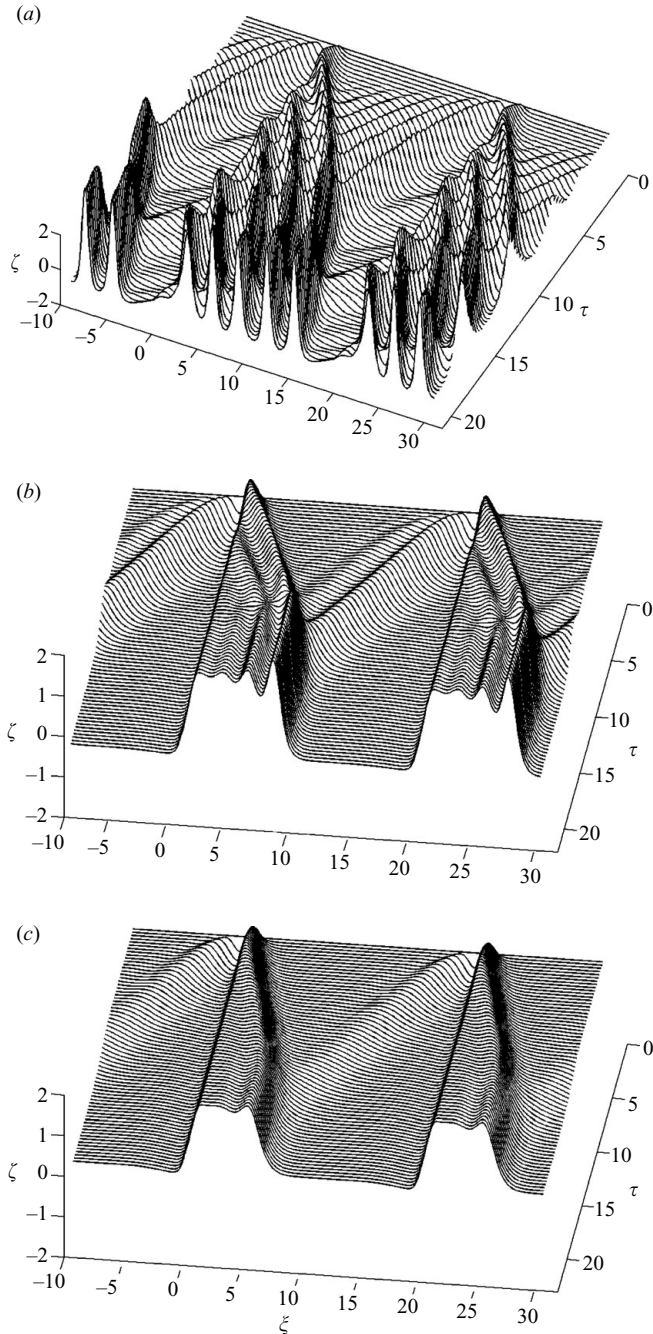
FIGURE 4. A caravan of ships separated by the distance $\Delta\xi = 20$: Ships are located in the range $\cdots$, $-1 < \xi < 1$, $19 < \xi < 21$, $\cdots$. (*a*) $D^2 = 0$, (*b*) $D^2 = 0.5$, (*c*) $D^2 = 1.0$. Common parameters are $\alpha = 0$, $\beta = 2$, $\ell = 1$.

The effect of the blockage parameter (β) is shown in figure 7. In general, a more slender ship (i.e. less blockage coefficient β) causes a smaller mound ahead and a shallower depression behind, as expected.
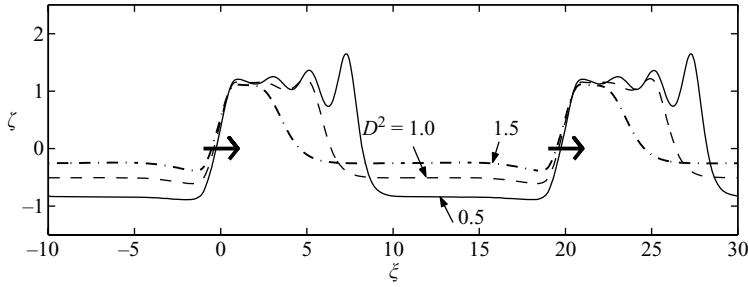
FIGURE 5. Effect of the roughness amplitude D^2 on the free surface between successive ships in a caravan separated at a distance $\Delta\xi = 20$. Input parameters are: $\ell = 1$, $\alpha = 0$, $\beta = 2$. Arrows represent the location and direction of ships.
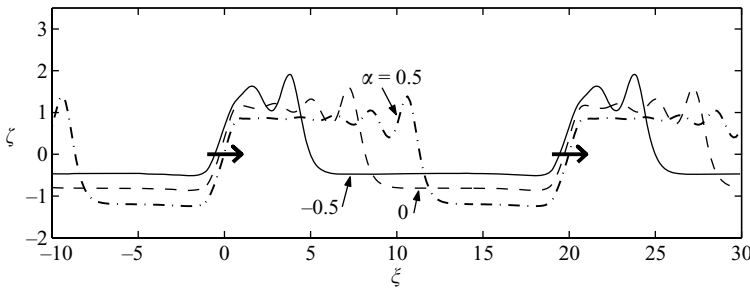
FIGURE 6. Effect of ship speed on the free surface between successive ships in a caravan separated by the distance $\Delta\xi = 20$. Input: $\ell = 1$, $\beta = 2$, $D^2 = 0.5$. Results plotted are for subcritical $\alpha = 0.5$, critical $\alpha = 0$, supercritical $\alpha = -0.5$. Arrows represent the location and direction of ships.
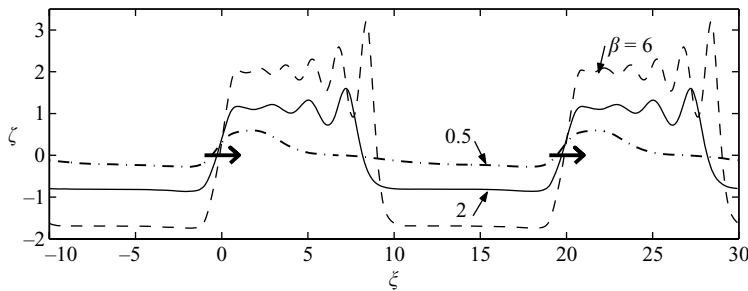
FIGURE 7. Effect of the blockage coefficient β on the free surface between successive ships in a caravan separated by the distance $\Delta\xi = 20$. Input parameters are: $\ell = 1$, $\alpha = 0$, $D^2 = 0.5$. Arrows represent the location and direction of ships.

In figure 8, the effects of separation distance on the steady wave pattern between ships are shown. For small separation ($\Delta\xi = 4$), the profile resembles a periodic train of cnoidal waves with a high crest in front and a shallow trough behind each ship. As the separation increases to $\Delta\xi = 10$, the high crest in front splits into two. Both the peak height and the trough depth behind decrease. By further increasing the ship separation to $\Delta\xi = 20$ and 30, the crest in front becomes a high plateau with more undulations; a long flat trough trails behind.
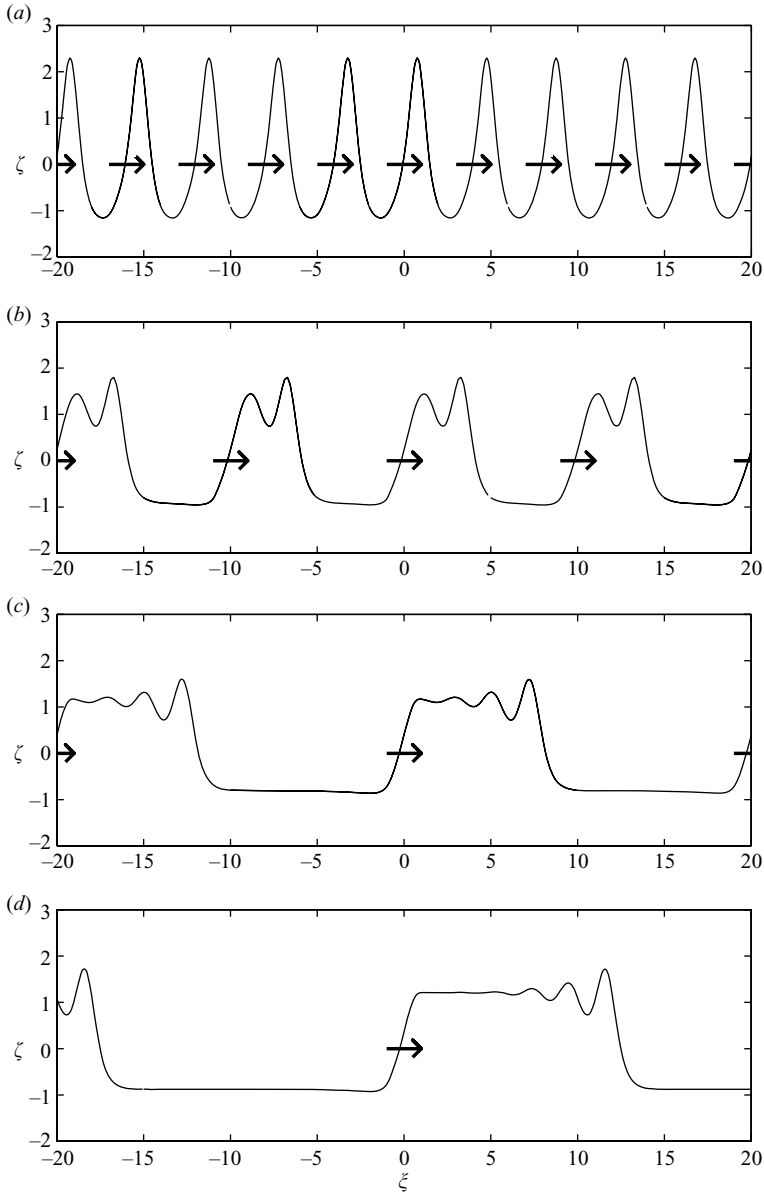
FIGURE 8. Effect of the separation distance between ships. Input parameters are $D^2 = 0.5$, $\alpha = 0$, $\beta = 2$, $\ell = 1$. (*a*) $\Delta\xi = 4$, (*b*) $\Delta\xi = 10$, (*c*) $\Delta\xi = 20$, (*d*) $\Delta\xi = 30$. Arrows represent the location and direction of ships.

7. Computed wave forces on a ship

From the numerical results of the preceding section, the free-surface displacement (hence pressure) on the ship hull varies roughly linearly from stern to bow. This can be used to derive crude qualitative estimates from (5.29) for comparison with the computed waves forces to be presented. Let us approximate ζ along the waterline to be linear in ξ,

$$\zeta \approx \bar{\zeta} + \tfrac{1}{2}\Delta\zeta\xi, \tag{7.1}$$
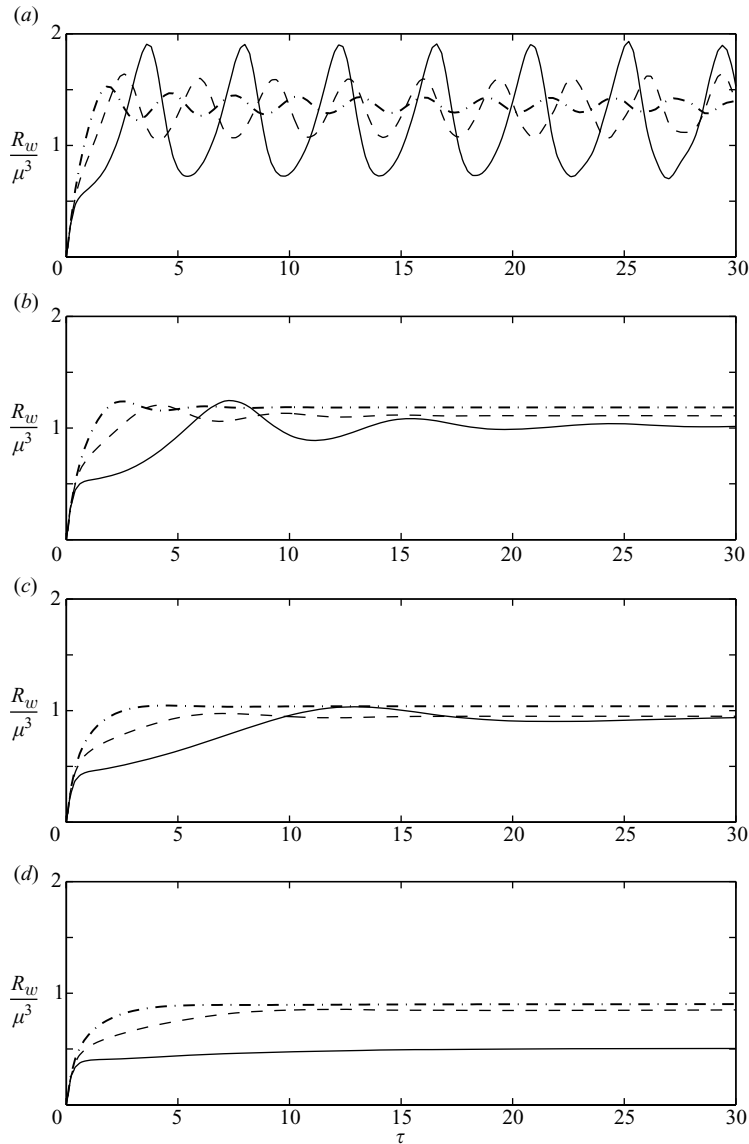
FIGURE 9. Resistance on a single ship in an infinite channel (cf. figures 1–3). Common parameters are $\beta = 2$, $\ell = 1$, (*a*) $D^2 = 0$, (*b*) $D^2 = 0.5$, (*c*) $D^2 = 1$, (*d*) $D^2 = 1.5$, for $\alpha = -0.5$ (———), $\alpha = 0$ (- - -), $\alpha = 0.5$ (– · –).

where $\bar{\zeta} \equiv [\zeta(-1, \tau) + \zeta(1, \tau)]/2$ denotes the mean and $\Delta\zeta \equiv \zeta(1, \tau) - \zeta(-1, \tau)$ denotes the difference, obtainable from computations. Assuming the ship cross-section to be semi-circular (results for a rectangular cross-section are quite similar), we have

$$\frac{dS}{d\xi} = -2\xi, \quad Y_w(\xi) = \sqrt{\frac{2(1 - \xi^2)}{\pi}}. \tag{7.2}$$

It is easy to show from (5.29) that

$$R_w \approx \frac{\mu^3}{2C_p} \frac{2}{3} \Delta\zeta, \quad F_z \approx \frac{\mu^3}{2C_w} \frac{\sqrt{2\pi}}{2} \bar{\zeta}, \quad M \approx \frac{\mu^3}{2C_w} \frac{\sqrt{2\pi}}{16} \Delta\zeta. \tag{7.3}$$
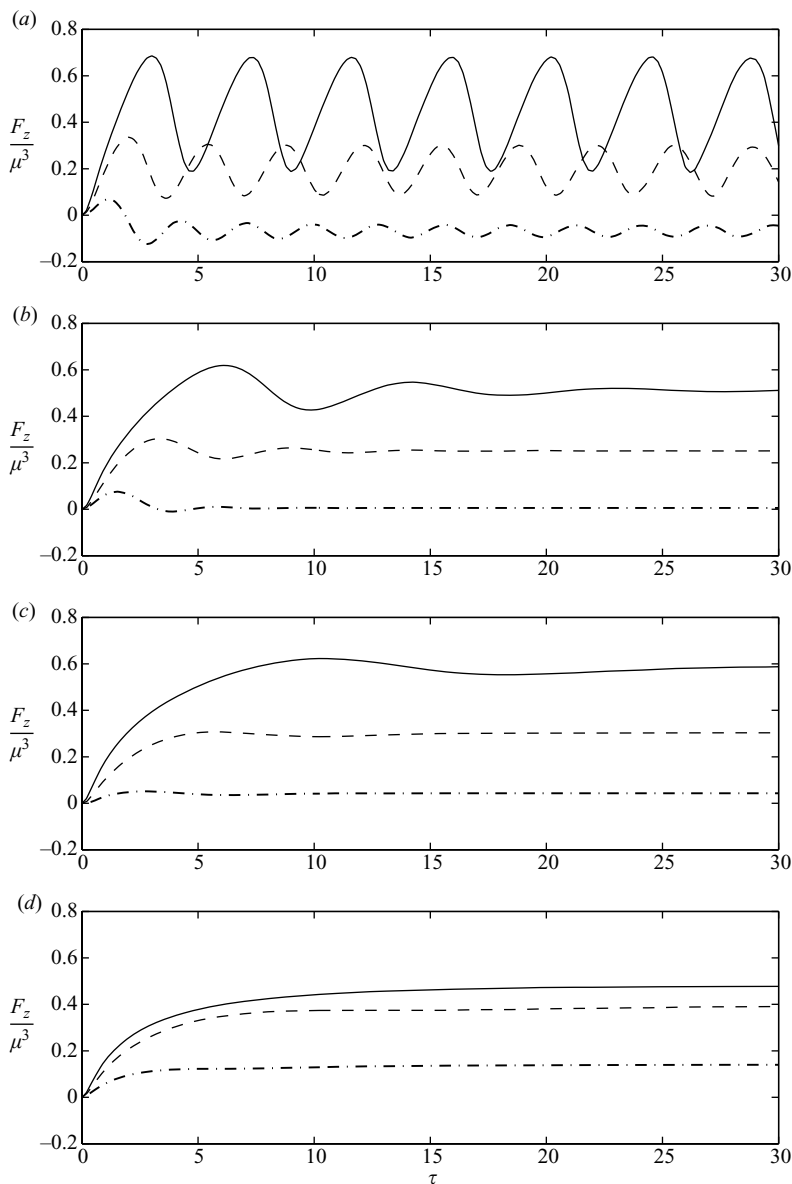
FIGURE 10. Vertical lift force on a single ship in an infinite channel (cf. figures 1–3).
Parameters and key as figure 9.

These estimates will be used shortly to interpret the computed forces. Note, in
particular, that the resistance and trimming moment are proportional to the drop of
water level from bow to stern, while the lift is proportional to the mean sea level. For
the chosen geometry of (6.1), $C_p = 2/3$ and $C_w = \pi/4$.

7.1. *One ship*

The transient evolutions of wave resistance on a single ship in an infinitely long
channel are shown in figure 9 for different ship speeds and heights of disorder. For
comparison, we recall that in the linearized approximation, the ship-induced motion
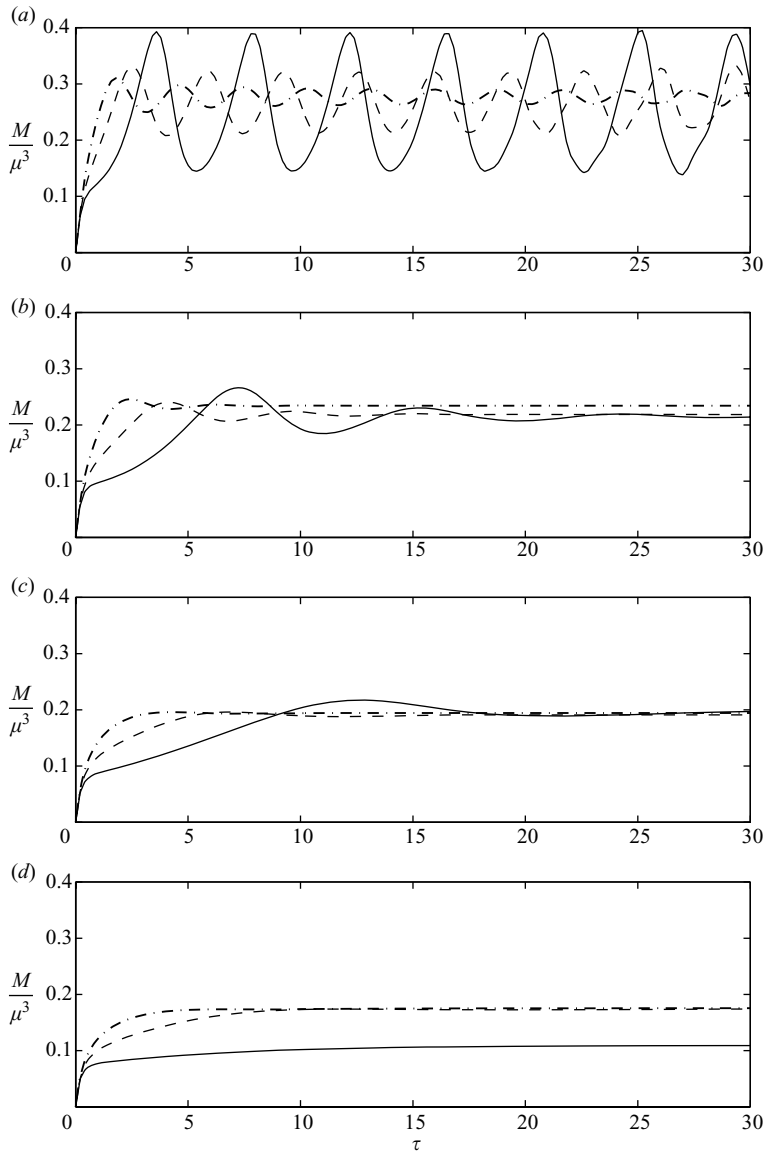
FIGURE 11. Trimming moment on a single ship in an infinite channel (cf. figures 1–3). Parameters and key as figure 9.

can be steady and the wave resistance is zero for subcritical speeds and finite for supercritical speeds (Tuck 1966). In a nonlinear theory for transcritical ship motion over a flat bed, upstream radiation of solitons renders the resistance oscillatory in time (Mei & Choi 1987). As the height of disorder increases, the oscillation diminishes, consistent with the surface profiles shown in figure 1. A tendency towards steady states is seen, but only after a long time, probably beyond the realm of accuracy of the present asymptotic theory. Vertical forces and trimming moments follow the same trend, as shown in figures 10 and 11. Note that for high roughness, the wave resistance is lower for a supercritical speed and higher for a subcritical speed. The same trend is found for a ship in a caravan, which will be discussed shortly.
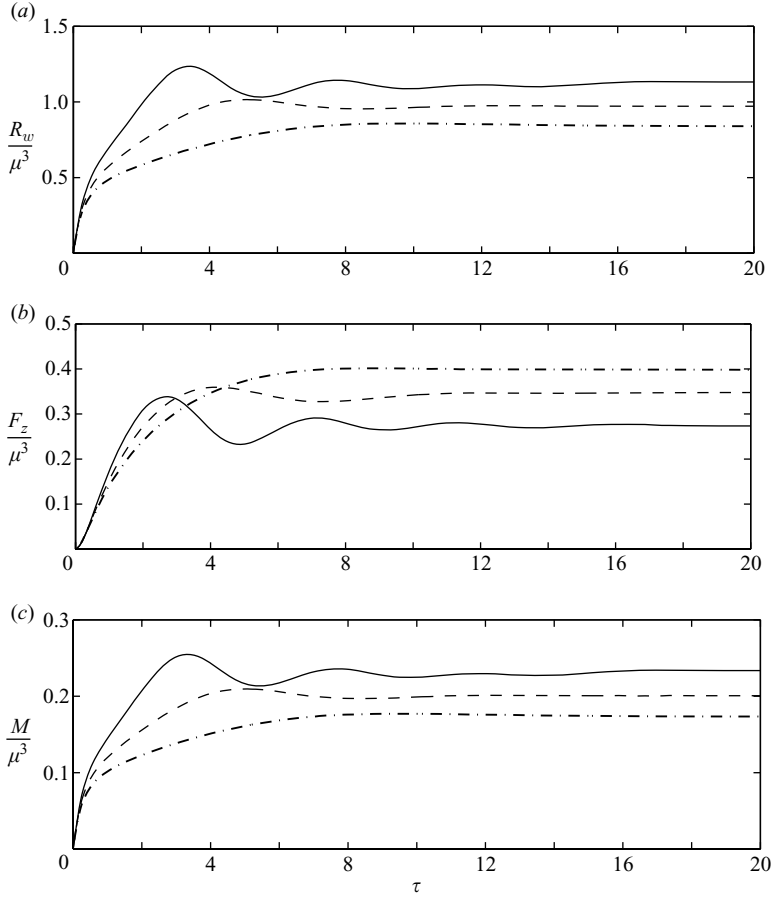
FIGURE 12. Effect of the roughness amplitude D^2 (cf. figure 5) on forces and moments on a ship in a caravan separated at $\Delta \xi = 20$. Parameters are $\beta = 2$, $\ell = 1$, $\alpha = 0$ for $D^2 = 0.5$ (——); $D^2 = 1.0$ (- - -); $D^2 = 1.5$ (– · –).

Based on the linearized shallow-water theory, Tuck (1966) found the vertical force at subcritical speeds to be downward, hence inducing sinkage, and cited some experimental evidence that the force is upward at supercritical speeds, hence inducing lift. According to the nonlinear theory, a slightly subcritical ship over a flat bed also experiences a downward vertical force (see for example Mei & Choi 1987, figure 5). Random bed roughness now amplifies the upward vertical force, hence lift can be experienced by subcritical and supercritical ships. The pitching (trimming) moment follows a similar trend which is similar to that of the resistance, as shown in figure 11. For a moderate bottom roughness, the trimming moment is almost independent of the speed.

7.2. *Many ships in tandem*

Wave forces on a ship in a caravan are shown in figure 12 for the critical speed only, but for different mean-square heights of bed roughness. All forces approach steady states at large times. As D^2 increases, the wave resistance and moment decrease while the lift increases. The reason can be understood from figure 5, which shows that an increase in the roughness does not change the height of the high water in front, but reduces the depth of depression behind, hence $\Delta \zeta$ decreases with increasing D^2,
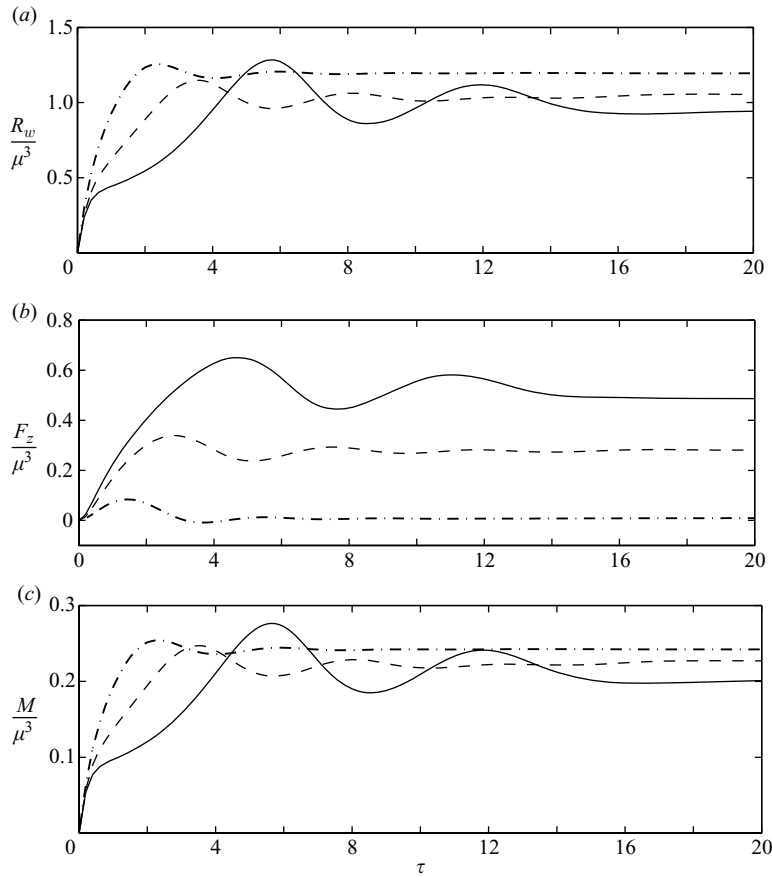
FIGURE 13. Effect of the ship speed (cf. figure 6) on forces and moments on a ship in a caravan separated at $\Delta\xi = 20$. Plots are for $\alpha = -0.5$ (——); $\alpha = 0$ (- - -); $\alpha = 0.5$ (– · –); Other parameters: $D^2 = 0.5$, $\beta = 2$, $\ell = 1$.

resulting in the reduction of wave resistance and trimming moment, in accordance with (7.3). On the other hand, the vertical force increases with roughness height. This is consistent with the increase in mean water level, consistent with (7.3).

Figure 13 shows the effect of the speed of ships over a bed of the same roughness. Again, higher speeds (smaller α) give lower wave resistance and moment, but greater lift at the steady state. From computations leading to figure 6, we find $\Delta\zeta = 1.9545$, 1.894 and 1.802 for $\alpha = 0.5$, 0 and -0.5, respectively. The decrease of R_w and M with increasing ship speed is indeed the result of decreasing $\Delta\zeta$; the increase of F_z is the consequence of increasing $\bar{\zeta}$, as seen in figure 6, again in agreement with (7.3).

Finally, figure 14 shows that as the separation distance increases, the wave resistance and the trimming moment decrease, as expected, but the vertical lift does not follow a monotonic trend.

8. Concluding remarks

It is known that when a ship advances near the critical speed in a channel with a smooth bottom, solitons are radiated periodically upstream. Our study here shows that if the channel bed is randomly uneven, in contrast to a flat bed, transient radiation is
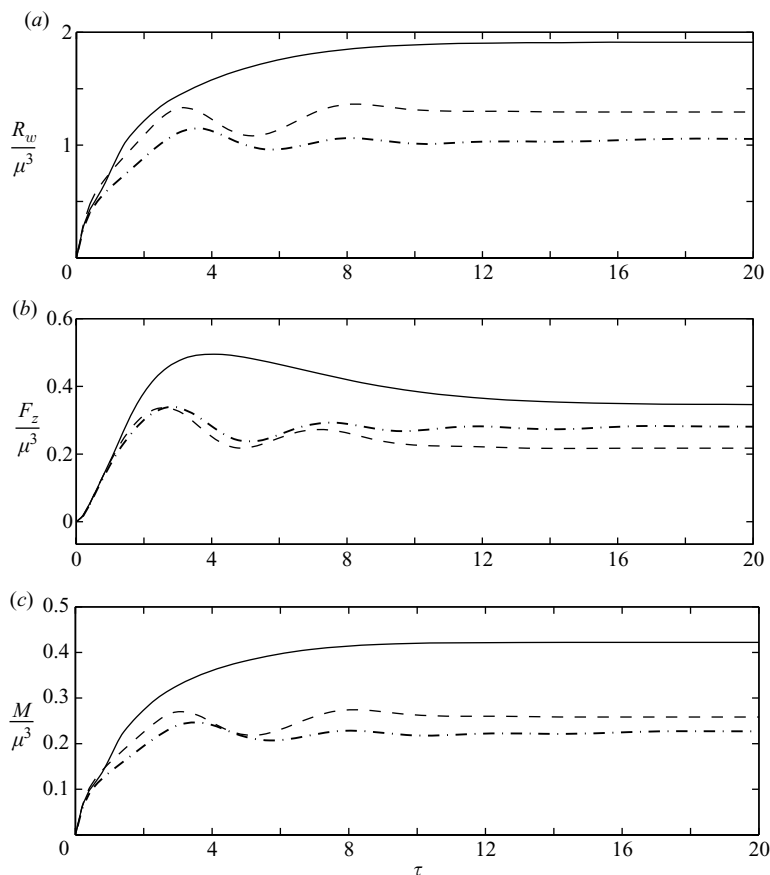
FIGURE 14. Effect of the separation distance (cf. figure 8) on a ship in a caravan. Plotted curves are $\Delta\xi = 4$ (——); $\Delta\xi = 10$ (- - -); $\Delta\xi = 20$ (– · –). Common parameters are $D^2 = 0.5$, $\alpha = 0$, $\beta = 2$, $\ell = 1$.

replaced by an expanding mound of high water pushed upstream. Surface undulations weaken, and forces and moments tend to become steady. If a caravan of identical ships advance at transcritical speed in the channel, transient waves can be totally damped, leading to a steady train of high waters between ships. In rivers, ships are more likely to cruise at high speed only if the river is much wider than is assumed here. In that case, waves in the wake must be two-dimensional. Experimental confirmation in a towing tank and extension of the present theory by adding Burgers-like terms to the forced Kadomtsev–Petviashvili equation are both worthwhile. Of possible interest to oceanography is the effect of random depth fluctuations on tide-induced solitons in a narrow strait with coastal indentations, protrusions, sills or ridges. Interesting changes from the case of one or few sills or ridges over a smooth bed (Baines 1995; Melville & Helfrich 1987; Cummins *et al.* 2003) may be expected.

REFERENCES

AKYLAS, T. R. 1984 On the excitation of long nonlinear water waves by a moving pressure distribution. *J. Fluid Mech.* **141**, 455–466.

ALAM, M.-R. & MEI, C. C. 2007 Attenuation of long interfacial waves over a randomly rough seabed. *J. Fluid Mech.* **587**, 73–96.

BAINES, P. G. 1995 *Topographic Effects in Stratified Flows*. Cambridge University Press.

CHEN, X. N. & SHARMA, S. D. 1995 A slender ship moving at a near-critical speed in a shallow channel. *J. Fluid Mech.* **291**, 263–285.

CHOI, H. S. & MEI, C. C. 1989 Wave resistance and squat of a slender ship moving near the critical speed in restricted water. *Proc. 5th Intl Conf. on Numerical Ship Hydrodynamics,* pp. 439–454.

COLE, S. L. 1985 Transient waves produced by flow past a bump. *Wave Motion* **7**, 579–587.

CUMMINS, P. F., VAGLE, S., ARMI, L. & FARMER, D. M. 2003 Stratified flow over topography: upstream influence and generation of nonlinear internal waves. *Proc. R. Soc. Lond.* A **459**, 1467–1487.

DUFFY, D. G. 2001 *Green's Functions with Applications*. Chapman & Hall/CRC.

ERTEKIN, R. C., WEBSTER, W. C. & WEHAUSEN, J. V. 1986 Waves caused by a moving disturbance in a shallow channel of finite width. *J. Fluid Mech.* **169**, 275–292.

GRATALOUP, G. L. & MEI, C. C. 2003 Localization of harmonics generated in nonlinear shallow water waves. *Phys. Rev.* E **68**, 026314.

HAMER, M. 1999 Solitary killers. *New Sci.* **163**, 18–19.

LI, Y. & SCLAVOUNOS, P. D. 2002 Three-dimensional nonlinear solitary waves in shallow water generated by an advancing disturbance. *J. Fluid Mech.* **470**, 383–410.

MEI, C. C. 1986 Radiation of solitons by slender bodies advancing in a shallow channel. *J. Fluid Mech.* **162**, 53–67.

MEI, C. C. & CHOI, H. S. 1987 Forces on a slender ship advancing near the critical speed in a wide channel. *J. Fluid Mech.* **179**, 59–76.

MEI, C. C. & HANCOCK, M. J. 2003 Weakly nonlinear surface waves over a random seabed. *J. Fluid Mech.* **475**, 247–268.

MEI, C. C. & LI, Y. 2004 Evolution of solitons over a randomly rough seabed. *Phys. Rev.* E **70**, 016302.

MELVILLE, W. K. & HELFRICH, K. R. 1987 Transcritical two-layer flow over topography. *J. Fluid Mech.* **178**, 31–52.

PIHL, J. H., MEI, C. C. & HANCOCK, M. J. 2002 Surface gravity waves over a two-dimensional random seabed. *Phys. Rev.* E **66**, 016611.

THEWS, J. G. & LANDWEBER, L. 1935 The influence of shallow water on the resistance of a cruiser model. *US Experimental Model Basin Report 408, Washington, DC, Navy Yard*.

TUCK, E. O. 1966 Shallow-water flows past slender bodies. *J. Fluid Mech.* **26**, 81–95.

WU, D. M. & WU, T. Y. 1982 Three-dimensional nonlinear long waves due to moving surface pressure. In *Proc. 14th. Symp. Naval Hydrodyn.* pp. 103–129.

ZHANG, D. H. & CHWANG, A. T. 2001 Generation of solitary waves by forward- and backward-step bottom forcing. *J. Fluid Mech.* **432**, 341–350.